

Response linearity of Nb tunnel junction detectors for photon energies from 1.5 to 6.4 keV

N. Rando,^{a)} A. Peacock, A. van Dordrecht, P. Hübner, and P. Videler
*Astrophysics Division, Space Science Department of the European Space Agency, ESTEC,
NL-2200 AG Noordwijk, The Netherlands*

J. Salmi and I. Suni
Technical Research Centre of Finland, Semiconductor Laboratory, Espoo, Finland

(Received 4 January 1994; accepted for publication 2 May 1994)

Recent experimental results show a linear energy response in high quality Nb-Al-AIO_x-Nb superconducting tunnel junction detectors for photon energies between 1.5 and 6.4 keV. The experimental data are based on both direct x-ray illumination and on the escape and re-absorption of fluorescent photons created in the junction electrodes and in the silicon substrate. The observed linearity of the energy response raises questions on the validity of some theoretical models which describe the relaxation process occurring in a superconducting thin film after x-ray photoabsorption. Such models generally predict nonlinear effects due to large quasiparticle number densities and short recombination times.

I. INTRODUCTION

Superconducting tunnel junction detectors (STJD's) are extensively investigated because of their potential intrinsic advantages in terms of energy resolution. Their fundamental properties have been discussed in detail elsewhere.¹ The high energy resolution arises from the fact that, at x-ray energies, the number of charge carriers created by the photoabsorption in a superconductor is of order 10⁶, about 1000 times more than in a semiconductor. The number of charge carriers N_0 produced by a photon of energy γ can be written as $N_0 = \gamma/\epsilon$, where ϵ is the mean energy necessary to create a single charge carrier. The intrinsic full width half maximum (FWHM) resolution of the detector is then R_0 (eV) = $2.355\sqrt{F\epsilon\gamma}$, where F is the Fano factor. In niobium, theoretical models indicate $F=0.22$ and $\epsilon=2.64$ meV, corresponding to $R_0=4.4$ eV at $\gamma=6$ keV.² The actual number of charge carriers N detected in the junction through tunneling can be approximated as:

$$N/N_0 = \frac{\tau_c^{-1}}{\tau_c^{-1} + \tau_r^{-1} + \tau_{\text{loss}}^{-1}}. \quad (1)$$

Here τ_c is the confinement time in one of the films, τ_r the quasiparticle lifetime, and τ_{loss} a characteristic quasiparticle loss time associated with the device. The confinement time can be determined from the volume of the junction electrodes, the barrier transmissivity, and the operating bias voltage.³ Quasiparticle loss mechanisms are associated with regions where the amplitude of the order parameter is reduced or suppressed: these areas act as trapping centers, inducing relaxation of the quasiparticles by phonon emission and subsequent recombination. The local reduction of the order parameter can be due to several mechanisms, such as magnetic field penetration in the superconducting thin films, electrode nonuniformities, or the localized deposition of a high energy density due to photoabsorption. The energy re-

sponse linearity is therefore dependent on whether τ_r and τ_{loss} are also a function of N_0 . If this were the case, the response of the detector could not be linear. This nonlinearity is a direct consequence of the Rothwarf-Taylor equations which describe the coupling between the quasiparticles and 2Δ phonons in the superconducting films.⁴ In order to investigate the linearity issue, a 50 μm square device was illuminated by highly collimated 6 keV x rays, for a total time of about 24 h. This long yet stable exposure time has allowed the identification of the fluorescence Nb escape lines from the niobium films as well as the fluorescent lines from the substrate. The absorption of an x-ray photon of energy $\gamma=6$ keV in Nb produces the emission of a primary electron from the L subshell, with an energy $E_p = \gamma - E_{Li}$ and a mean range of 0.1 μm . Here E_{Li} is the i th subshell energy ($E_{LIII}=2.37$ keV). The subsequent Nb atomic relaxation can be either through a transition from a higher shell (M or N) to the L_i subshell with the emission of a fluorescent Nb L -shell photon γ_{Li} , or via a complex radiationless transition with emission of an Auger electron. The probability of these process occurring depends on the shell fluorescent yield w_L (about 7% in Nb). In the case of niobium, the fluorescent photon arises mainly from the LII-MIV and LIII-MV transitions, with energies γ_L of 2.26 and 2.17 keV, respectively. The probability that such a fluorescent photon is re-absorbed in the junction electrodes depends on the size and the thickness of the thin Nb films. If the photon is not absorbed, then only the residual energy $\gamma - \gamma_{Li}$ will be deposited in the junction. These residual escape lines around 3.64 and 3.73 keV, together with the Mn K_{α} , K_{β} lines and the K -shell fluorescent lines due to the substrate, have provided a measure of the device linearity between 1.5 and 6.4 keV.

II. DEVICE CHARACTERISTICS

The devices were fabricated using a modification of the standard Nb-Al-AIO_x-Nb trilayer process.⁵ Thermally oxidized silicon wafers covered with reactively rf-sputtered

^{a)}E-mail: nrando@astro.estec.esa.nl

Al₂O₃ were used as substrates. The SiO₂ and Al₂O₃ were 177 nm and 26 nm, respectively.

Nb and Al were dc magnetron sputtered in an Ar atmosphere of 0.44 Pa. The base pressure was better than 10⁻⁵ Pa. The wafers were mounted on water-cooled copper blocks. Particular care was taken to keep the back side of the wafers clean to ensure good thermal contact ion cleaning and sputter deposition. Before film deposition the surface was cleaned by *in situ* Ar ion-milling.

A double oxidized Nb-Al-AlO_x-Al-Nb structure was used as junction barriers.⁶ The base electrode Nb was first sputtered at a deposition rate of 1.1 nm/s followed immediately by the first Al film at a sputtering rate of 0.4 nm/s. Then the vacuum chamber was evacuated of Ar and backfilled with pure O₂ to a pressure of 40 Pa. The first oxidation step was carried out at room temperature for 1 h. Before sputter depositing the second Al layer the chamber was pumped down below 10⁻⁵ Pa. The second Al film was deposited at a rate of 0.15 nm/s and an oxidation step identical to the first one was repeated. After the subsequent pump down the Nb counter electrode was sputtered using the same parameters as for the base electrode. The thicknesses of the base electrode, the first Al layer, the second Al layer, and the counter electrode were 250, 7, 0.7, and 250 nm, respectively.

The junction sandwich was patterned in two steps. In the first step the base electrode was delineated by reactively ion etching (RIE) through the Nb films using SF₆ gas. The Al-AlO_x layers were etched in phosphoric acid.

Before the second patterning step an anodization mask layer of SiO₂ was grown by plasma enhanced chemical vapor deposition (PECVD) at 120 °C. The SiO₂ thickness was 50 nm and it was patterned in buffered HF to define the junction perimeter. The Nb counter electrode was then subsequently patterned using RIE. The junction edges were passivated by growing a 145 nm thick layer of anodic Nb₂O₅. After having stripped the SiO₂ mask the second patterning step was carried out to isolate the junction structures from each other. Finally a Nb layer with a thickness of 500 nm was sputtered to provide the base and counter electrode leads and the contact pads. Liftoff was used to pattern this layer and a 50 nm thick Au film e-gun evaporated on the contact pads.

Eight devices of different shape and area were isolated from the original junction sandwich. The results reported in this paper refer to a 50 μm square junction, whose basic characteristics are summarized in Table I. The leads width is equal to 5 μm.

The Josephson critical current could be suppressed to the nA level with a magnetic field (parallel to the junction electrodes) of about 200 G. The measured quality factor at 4.2 K corresponds to 31 mV, while, considering the large area of the device, the subgap current at the base temperature of 1.20 K is very low (leakage = 1.7 pA/μm²). The results reported in this paper are not unique to one junction, but the most representative of the chip.

III. THE X-RAY PERFORMANCE

The x-ray performance of the device has been investigated by means of a 25 mCi Fe⁵⁵ source, which emits two lines complexes, from Mn K_α at 5895 eV and from Mn K_β at

TABLE I. Device characteristics. $V_m = 2I_c/I_{sq}$ (@2 mV) in mV, with I_c measured maximum Josephson current.

Counter electrode area	A_c	2352 μm ²
Gap voltage	V_g	2.8 mV
Normal resistance	R_n	2.3 Ω
Dynamic resistance	R_d	50 kΩ
Measured critical current density	J_c	17 A/cm ²
Bias voltage	V_b	0.20–0.25 mV
Subgap current at V_b at 1.2 K	I_{sg}	1.0–4.0 nA
Confinement time ($V_b = 0.2$ mV)	τ_c	13.7 μs
Quality parameter (at 4.2 K)	V_m	31 mV

6401 eV, with an intensity ratio of 8.4:1. The experimental set-up has been described in detail elsewhere.² Experiments have been conducted using two different configurations: (a) with uncollimated illumination over a 2500 μm diameter area, (b) with highly collimated illumination over a 7 μm diameter area.^{7,8} This latter configuration was used in order to demonstrate the existence of position dependence mechanisms responsible for a severe degradation of the detector energy resolution.

A. Uncollimated configuration

The spectrum obtained in the uncollimated configuration is shown in Fig. 1: the measurements were taken at a temperature of 1.20 K. A test pulser was also used in order to measure the electronics noise which was found to be 3500 electrons, equivalent to 32 eV at the Fe⁵⁵ main K_α peak energy. A few features are worthy of mention: (i) the number of counts at low energies is very low in comparison with previous results,^{1,2,8} indicating that the two buffer layers (1770 Å of SiO₂ and 260 Å of Al₂O₃) efficiently stop the detection of indirect events from the substrate⁹; (ii) the energy resolution is clearly degraded, with a significant and uniform broadening of the main peaks; note the count rate from the source was sufficiently low so as to play no role in the spectrum distortion; (iii) a low energy peak is recognizable as a result of Si, K_α fluorescence at 1.74 keV. The ob-

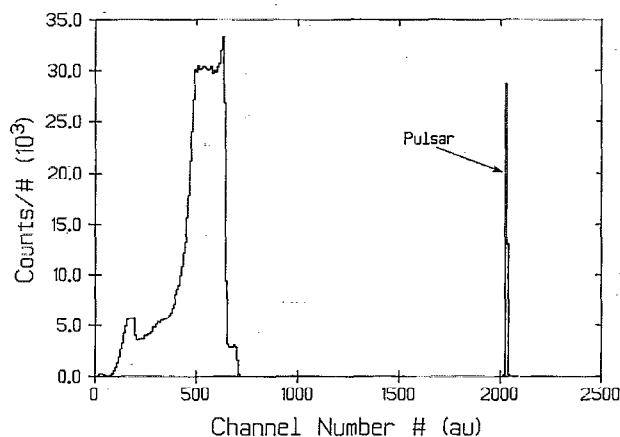


FIG. 1. Fe⁵⁵ spectrum obtained in the uncollimated configuration with the 50×50 μm device. The test pulse peak allows the evaluation of the electronics noise.

served broadening of the main peak is a clear indication of reduced quasiparticle diffusion throughout the junction during the confinement time: a rapid charge diffusion in the system would in fact compensate significantly for any spatial variation associated with the photon absorption site, ensuring a more uniform detector response and higher spectroscopic performance. This interpretation is also reinforced by the results of the collimated experiment.

B. Collimated configuration

In order to isolate such position dependent effects responsible for the observed degradation, a second experiment has been performed on the same device, this time making use of a collimation pinhole of $5\ \mu\text{m}$ diameter. The experimental configuration has been described elsewhere^{7,8} and allows the illumination of a selected area of the device as small as a circle $7\ \mu\text{m}$ in diameter. In this case the pinhole has been positioned at the center of the junction counter electrode and, given the large area of the device ($50\times 50\ \mu\text{m}^2$), it has been possible to confine the photon illumination to a relatively small and central area of the detector. This eliminates any contribution from the detector leads or from the underlap existing between base and counter electrode. In order to obtain good statistics, data were accumulated over a period of 24 h. The results of this test are represented in Fig. 2: again all the measurements were taken at 1.20 K, with the only difference being given by a different coupling between detector substrate and the cryostat cold finger. In this case in fact, the device substrate must be fixed to a supporting copper board by means of Ag paint. Again, some important features are: (i) the overall cleanness of the spectrum and the energy resolution of the device are greatly improved in comparison with Fig. 1; (ii) the charge output is a factor of 2 lower than in the previous configuration; this reduction can be explained in terms of a position dependent detector responsivity and in terms of the different substrate to cold finger coupling; (iii) the main K_α and K_β structures are clearly resolved, with no evident distinction between base and counter electrode contribution; the energy resolution corresponds to about 260 eV, including the electronic noise which is equal to about 63 eV at the Fe^{55} K_α peak energy; (iv) at least two additional peaks are detectable at 1.74 keV and 3.64–3.73 keV. The first line can be identified with fluorescent Si K_α from the substrate, while the second broadened line complex represents the mean Mn K_α Nb escape radiation, arising from the main L subshell transitions. Evidence for a third line at very low intensity, arising from the AlO_x buffer layer and producing a fluorescent line at 1.49 keV, is also found. The spectrum of Fig. 2 demonstrates the presence of a remarkable spatial dependence in the detector response: illumination over a small area produces in fact a much better defined spectrum, while the uncollimated performance is the result of different responses at different absorption sites in the detector. Since the diameter of the central illuminated area is $7\ \mu\text{m}$, spatial variations must occur over a larger scale, eventually involving the detector edges. Such response non-uniformities have been recently confirmed and imaged in Nb STJD's by means of low temperature scanning electron microscope techniques.¹⁰ This result also indicates that quasi-

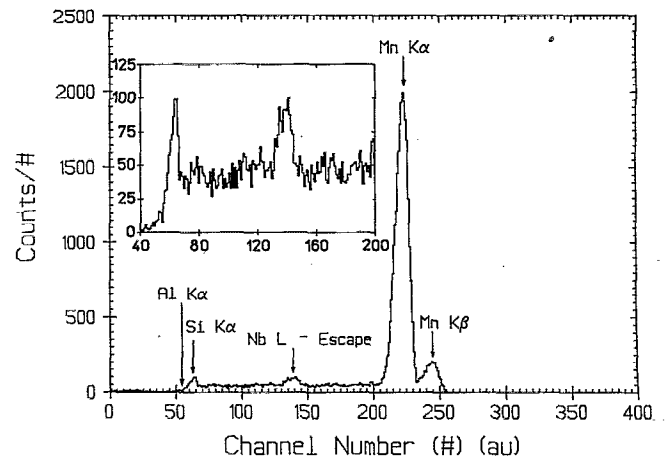


FIG. 2. Fe^{55} spectrum obtained in the collimated configuration (aperture of $5\ \mu\text{m}$ diameter) with the same $50\times 50\ \mu\text{m}$ device. The inset shows the detail of the fluorescence and escape lines. The broader peak, at channel number 140, corresponds to the the Nb escape lines at 3.64 and 3.73 keV.

particles diffusion is limited to a small volume of the absorbing film, possibly related to the grain size of the polycrystalline films. If this is the case, a relatively high energy density would be expected at each photoabsorption site, with correspondingly high quasiparticle number densities.

In both the experimental configurations, it is not possible to identify a separate contribution from base and counter electrode: this can be explained by the fact that since the films have the same thickness, their confinement times are expected to be very similar. Moreover, base and counter electrode are both polycrystalline and therefore similar diffusion transport properties are also envisaged. This element is partly responsible for the poor resolution still observed in the collimated configuration: a slightly different response from each film would introduce an additional resolution degradation.

IV. ENERGY RESPONSE LINEARITY

Figure 3 shows the linearity of the detector response as measured from the five main peaks recognizable in the spectrum, at 1.49, 1.74, 3.64–3.73, 5.89, and 6.4 keV: despite a reduced quasiparticle diffusion throughout the junction electrodes, the best fit straight line indicates a response linearity better than 1%.

This result seems to contradict somewhat, at least for Nb, those recent theoretical models^{11,12} proposed to describe the photoabsorption process in superconducting thin films and that assume the presence of high quasiparticle number densities in a limited volume region and corresponding significant nonlinear effects due to high recombination rates. This linearity property is particularly interesting given the long confinement time of this specific device ($\tau_c=13\ \mu\text{s}$). Experimental evidence of nonlinearity has been found in Sn devices,¹³ while it is suspected in Al STJD's.¹⁴ In the soft x-ray regime the energy deposited by photoabsorption will mainly go in to the electronic system, since only a few nuclear displacements occur at photon energies below 100 keV. The latter would of course give rise to a corresponding

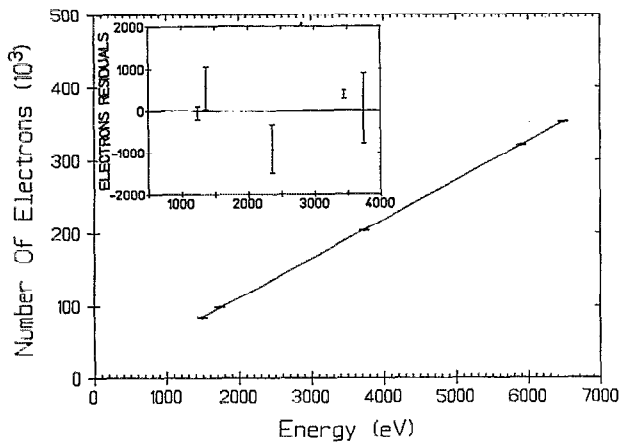


FIG. 3. Charge output as a function of the photon energy between 1.5 and 6.4 keV. The data refer to the collimated experiment. The solid line is the best fit solution based on the linearity assumption. The inset shows the best fit residuals.

population of energetic phonons. In niobium, the absorption of a photon at $\gamma=6$ keV will produce the emission of a primary electron from the atom L -shell, with energy of about 3.5 keV; this primary electron initiates an inelastic scattering process which produces secondary electrons and that will be concluded when the energy of the primary electron is indistinguishable from the other electrons (energy of order 1 eV). The volume in which this cascade process occurs has been proposed to be a cylinder of length equal to the primary electron range R_e (equal to $0.17 \mu\text{m}$ in Nb at 6 keV) and of radius given by 20 times the average secondary electron range (equal to 0.89 nm in Nb). According to this scenario,¹¹ the energy would be confined within a volume of about $4.2 \times 10^{-7} \mu\text{m}^3$, corresponding to an energy density of order $10^{10} \text{ eV}/\mu\text{m}^3$, which exceeds the pairs condensation energy density by a factor 10^5 . In other words, nonlinearities might be expected at photon energies well below 10 keV. Given the result of Fig. 3, we must conclude that the spatial evolution of the absorbed energy may differ from that previously envisaged. The predicted nonlinearity mechanisms could well be related to the quality of the thin films, specifically the grain size and the structure. It must be stressed that the nonlinearity is primarily based on the parameter τ_r of Eq. (1). If however $\tau_r \ll \tau_{\text{loss}}$, then a linear response would be expected. If there is therefore another mechanism responsible for the quasiparticle loss which is not dependent on the energy density, then the response could be linear. This conclusion is reinforced by the fact that these results have been obtained with a device characterized by a long confinement time and therefore far more sensitive to any self recombination or trapping mechanism. Of course models in which the energy gap in the absorption region has been suppressed, such that locally a normal metal exists, are a possibility. In this case the concept of quasiparticles on which the Rothwarf–Taylor equations are based simply would not apply.

The presence of a magnetic field is also expected to increase the quasiparticle loss rate due to magnetic flux entry

and trapping. Experimental results have confirmed a net reduction of the order parameter in superconducting films as a function of the applied field. It has also been shown that this effect may introduce a further loss term to the Rothwarf–Taylor modeling of the evolution of the nonequilibrium quasiparticle population.^{15,16} In our measurements the applied magnetic field was about 200 G. While we cannot exclude the fact that the applied field could be partly responsible for the observed spatial nonuniformities, especially at the detector edges,¹⁵ such effects do not seem to affect the energy linearity of the system.

V. CONCLUSIONS

An energy response linearity better than 1% has been found in Nb-Al-AlO_x-Nb STJD's for photon energies between 1.5 and 6.4 keV and at a temperature of 1.2 K. This result would seem to contradict those theoretical models which predict high self recombination rates and potential nonlinearities even in the soft x-ray regime. High collimation experiments have shown the presence of remarkable nonuniformities in the spatial response of the detector, nonuniformities which are certainly responsible for a considerable degradation of the spectroscopic performance of this device and which occur at a few μm^2 level. It is clear from these results that the overall junction response as well as the device linearity are strongly related to the structure of the Nb films.

- ¹N. Rando, A. Peacock, C. Foden, A. van Dordrecht, J. Lumley, and C. Pereira, *J. Appl. Phys.* **73**, 5098 (1993).
- ²N. Rando, A. Peacock, A. van Dordrecht, C. Foden, R. Engelhardt, B. Taylor, J. Lumley, and C. Pereira, *Nucl. Instrum. Methods A* **313**, 173 (1992).
- ³P. de Korte, M. van Berg, M. Bruijn, M. Frericks, J. le Grand, J. Gijsbertsen, E. Houwman, and J. Flokstra, *Proc. SPIE Conf. (San Diego)* **1743**, 24 (1992).
- ⁴A. Rothwarf and B. Taylor, *Phys. Rev. Lett.* **19**, 27 (1967).
- ⁵H. Seppä, M. Kiviranta, A. Satrapinski, L. Grönberg, J. Salmi, and I. Suni, *IEEE Trans. Appl. Supercond.* **3**, 1816 (1993).
- ⁶E. Houwman, D. Veldhuis, J. Flokstra, and H. Rogalla, *J. Appl. Phys.* **67**, 1992 (1990).
- ⁷W. Fischer, N. Rando, A. Peacock, and R. Venn, *Rev. Sci. Instrum.* **65**, 603 (1994).
- ⁸N. Rando, C. Foden, A. Peacock, and A. van Dordrecht, *IEEE Trans. Appl. Supercond.* **3**, 2080 (1993).
- ⁹Y. Levinson, in *Nonequilibrium Phonons in Nonmetallic Crystals*, edited by Eisenmenger and Kaplyanskii (North Holland, Amsterdam, 1986), Vol. 16, p. 51.
- ¹⁰S. Lemke, F. Hebrank, F. Fominaya, R. Gross, R. Huebener, N. Rando, A. van Dordrecht, P. Huebner, P. Videler, and A. Peacock, *Physica B* **194**, 1663 (1994).
- ¹¹D. van Vechten and K. S. Wood, *Phys. Rev. B* **43**, 12852 (1991).
- ¹²D. van Vechten, K. Wood, M. Lovellette, and G. Arnold, in *Proceedings of Low Temperature Detectors for Neutrinos and Dark Matter IV*, edited by N. Booth and G. Salmon (Editions Frontières, Gif-sur-Yvette, 1992), p. 347.
- ¹³W. Rothmund, C. Hagen, and A. Zehnder, in *Proceedings of the Workshop on Superconducting Tunnel Junction Detectors for X-rays*, edited by A. Barone, R. Cristiano, and S. Pagano (World Scientific, Singapore, 1991), p. 196.
- ¹⁴P. Brink, D. Goldie, C. Patel, N. Booth, and G. L. Salmon, *J. Low Temp. Phys.* **93**, 555 (1993).
- ¹⁵K. Wood and D. van Vechten, *Nucl. Instrum. Methods A* **314**, 86 (1992).
- ¹⁶E. Houwman, A. Golubov, J. Gijsbertsen, J. Flokstra, H. R. J. le Grand, M. P. Bruijn, and P. de Korte, *J. Low Temp. Phys.* **93**, 677 (1993).